Int. J. Solids Structures Vol. 14, pp. 941–957

0020-7683/78/1101-0941/$02.00/0

THE RAPIDLY HEATED RIGID-PLASTIC CANTILEVER

E. W. PARKES
The City University, St. John Street, London EC1V 4PB, England

(*Received* 15 *February* 1978; *in revised form* 8 *May* 1978)

Abstract—The concept of the expanding and contracting hinge produced by rapid thermal curvature is applied to the detailed analysis of a cantilever. In addition to a general study of the modes of deformation, the accelerations velocities and displacements are determined for a specific case. Although for the example chosen, less than 10% of the final plastic curvature occurs in the root hinge, a greatly simplified "strong beam" analysis which constrains all plastic deformation to the root hinge gives a tip deflection only 6% less than the original value. The paper includes a discussion of the conditions which must be satisfied such that longitudinal inertia effects and elastic deflexions do not invalidate the analysis when it is applied to real materials.

NOTATION

A	parameter determining the rapidity of heating
av	suffix denoting average value
B	$(\omega l/2\pi)(\rho/E)^{1/2}$
b	breadth of cantilever
d	depth of cantilever
E	Young's modulus
e, c	suffices denoting expansion and contraction phases of hinge
F	stress factor
h	x_h/l
h	suffix denoting boundary of expanding or contracting hinge
h^+	suffix denoting section just outside hinge
h^-	suffix denoting section just within hinge
i	suffix denoting value at beginning of current regime of behaviour
K	time dependent function in equation for thermal strain
l	length of cantilever
M	bending moment
max	suffix denoting maximum value
M_p	full plastic moment
P	longitudinal force
P_p	full plastic force
m	mass per unit length
S	shear force
t	time
$t_1 \ldots t_6$	times defining boundaries between zones of behaviour
t_x	time at which section x enters hinge
w	deflexion
w_{pi}	deflection at beginning of current regime of behaviour due to some previous history of plastic deformation
x	coordinate along cantilever, measured from the root
y	coordinate of depth in cantilever, measured from mid-height
β	$\{(1-\gamma)(33-\gamma)\}^{1/2}$
γ	$72M_p/m\bar{\chi}_T l^4$
ϵ_T	thermal strain
θ	dw/dx
θ_0	value of θ at $x = 0$
κ	$A/B^2\mu^2$
λ	constant in equation for thermal strain
μ	l/d
Ω	B/μ
ρ	density
σ_y	yield stress
$\dot{\phi}$	discontinuity in angular velocity at x_h
χ_T	thermal curvature $= (12/d^3)\int_{-(1/2)d}^{(1/2)d} \epsilon_T y \, dy$
ω	parameter defining period of heating pulse $(= 2\pi/\omega)$

1. INTRODUCTION

In a previous paper [1] it was shown that in any rigid-plastic beam subjected to sufficiently rapid thermal curvature there would develop expanding and contracting plastic hinges occupying finite lengths of the beam. A general theory was given which demonstrated the different

physical characteristics of the expansion phase, during which angular velocity is a continuous function along the beam, and the contraction phase, when angular velocity is discontinuous. The purpose of this previous paper was partly to demonstrate the necessity for the existence of non-discrete hinges, and partly to explore the possible definition of thermal curvature for an inelastic beam. A brief application of the theory was given to show the zones of behaviour which can occur in a free beam, but no attempt was made to analyse the deformations.

The present paper uses the general ideas of the earlier work and applies them to a detailed study of the cantilever. The cantilever was chosen because it is the structure which has attracted greatest attention in the literature of dynamic plasticity. The reason for this is probably that it is a well-defined system for experimental work. In any other type of beam (with the exception of the free beam, which introduces experimental difficulties) there is always some possibility of axial restraint and thus interaction between bending and end-load plasticity.

The first application of dynamic plastic theory to an important practical problem was the design in 1940 of the "Morrison" table shelter[2]. This shelter was intended to resist the collapse of part of a building. The striking mass was large and its velocity low, so that the plastic hinges formed were static. The earliest work on dynamic plasticity which implies hinge movement is that of Bohnenblust on the infinitely long beam subjected to a transverse impact of constant velocity. This work was carried out in a defence context in 1943 but was not published until seven years later[3]. Bohnenblust's analysis could incorporate any form of moment-curvature relationship and good agreement was obtained with experiments on mild steel and annealed copper. A rigid-plastic analysis of the long beam under transverse impact was given by Conroy[4]. The encastré beam of finite length was discussed by Parkes[5, 6]: these papers include experimental work on steel, brass and duralumin specimens designed to elucidate strain-rate effects.

The next type of structure to be considered in the development of rigid-plastic theory seems to have been the free beam. Lee and Symonds[7] and Symonds[8] discussed a free beam subjected to a central transverse force which varied with time in a specified manner–triangular, rectangular or half sine wave forms were employed. Symonds and Leth[9] dealt with the free beam in which the central impact was of constant velocity.

The first paper discussing a cantilever struck by a moving mass is that of Parkes[10]: experiments were carried out on mild steel cantilevers using both very heavy and very light strikers, and good agreement was obtained with theoretical predictions provided rate-of-strain effects were taken into account. Mentel[11] carried out experiments on cantilevers with attached tip masses, but very little of the deformation in his tests was attributable to travelling hinges. Bodner and Symonds[12] performed a series of tests on steel and aluminium alloy cantilevers to assess the importance of the factors which simple rigid-plastic theory ignores: elastic vibrations, shear deformation, extensional deformation, geometry changes, strain-rate and strain hardening effects. Bodner and Speirs[13] tested aluminium cantilevers whose tips were given an impulse by an explosive capsule. The tests, which were carried out at elevated temperatures, were compared with the original theoretical work of Parkes[10] and with later analyses by Bodner, Symonds and Ting which incorporated strain rate effects in the governing equations. As might be expected they found that the significance of strain rate increased with temperature.

Ting[14] gave an analysis for a cantilever made from a material having strain rate sensitivity. He assumed that strain rate is proportional to a power function of the stress in excess of the static yield stress. Comparisons were made with the experimental results from Bodner and Symonds[12]. He later[15] developed a large displacement theory for the cantilever and compared his results with the experiments of Parkes[10].

Hall, Al-Hassani and Johnson[16] carried out a very extensive experimental programme on the impulse loading of cantilevers. The methods of loading, all of which were stated to correspond to Parkes' "light" strikers, included magneto-motive loading, necessitating high electrical conductivity, and thus aluminium or copper specimens, contact explosives and bullets. Detailed comparisons were made with Parkes[10] theory in all cases, including his expression for the length of the short straight portion near the tip in the case of bullet loading.

Recent developments in the study of impulsively loaded cantilevers have included work by Hashmi, Al-Hassani and Johnson[17] using lumped parameter models to investigate very large

deformations: comparison was made with experiments. A quite different approach has been that of Martin[18] who derived theorems providing a lower bound on the response time and an upper bound on the deflection for an impulsively loaded structure: he found that on comparing his work with Parkes[10] the response time was accurate but the deflection bound became progressively less accurate for the lighter strikers. The idea of bounds has been developed further by Symonds and Chan[19]. Fibre-reinforced rigid-plastic cantilevers have been studied by Jones[20], who compared his results with Parkes[10] and Bodner and Symonds[12].

There is an important distinction to be drawn between all of the work on cantilevers described above, and that in the present paper. When a beam is subjected to plasticity as the result of rapid thermal curvature, this can only be produced by heating, since the processes of cooling cannot take place sufficiently quickly. As a result, rapid thermal curvature is always accompanied by longitudinal inertia force in the beam. This longitudinal force may affect the analysis in two ways: it may reduce the value of the yield moment; and if the deflexions are sufficiently large it may contribute significantly to the bending moment. In Sections 2–5 of the paper we shall develop the analysis ignoring longitudinal inertia effects. In Section 6 we shall consider what conditions must be satisfied such that these effects are negligible, and in the same section we shall investigate the validity of the usual assumption of dynamic plasticity theory, that elastic deflexions may be ignored.

The present paper begins with a study of the modes of behaviour of the cantilever subjected to rapid thermal curvature. The analysis draws substantially on the work on the free beam in Parkes[1], but more detailed consideration is given to the case of the instantaneously created extensive hinge, which is of greater significance for the cantilever than for the free beam. The zones of behaviour as functions of the rapidity of heating and of time are next determined for a sinusoidal heating pulse, and then a detailed analysis of the accelerations, velocities and displacements of the cantilever is given for a specific case. The development of expanding and contracting hinges and of instantaneously created extensive hinges is clearly shown. For the particular case chosen, the final plastic curvature occurs over nearly one quarter of the length of the cantilever, less than 10% of it being in the root hinge.

The full analysis of the cantilever subjected to rapid thermal curvature is complicated, and extensive numerical calculations are needed to determine the final deformations. It seems natural therefore to look for simplifying assumptions which will reduce the labour involved without introducing unacceptable errors. One such assumption which has been investigated in the present paper is the concept of the strong beam, in which all deformation takes place in the root hinge, the rest of the cantilever remaining rigid even though the bending moment exceeds the fully plastic moment. For the specific example, this approach led to a tip deflection which was some 6% less than the value given by the full analysis.

The paper ends with discussions of longitudinal inertia forces and elastic deformations, and the conditions which must be satisfied such that their effects do not invalidate the analysis.

2. GENERAL ANALYSIS

2.1 *The modes of behaviour*

We consider a rigid-plastic beam of uniform section subjected to a thermal curvature χ_T which varies with time but not with position. The assumptions relating to the existence and determination of χ_T are discussed in the appendix to Parkes[1], and it is defined in the Notation. The beam section and the manner of support are supposed to be such that longitudinal inertia effects are unimportant compared with bending phenomena: the conditions under which this will be true are discussed in detail in Section 6. Then the thermal curvature will produce a shear force S, a bending moment M and a deflexion w at section x of the beam, where x is a co-ordinate measured from some fixed position. The sign conventions for χ_T, S, M, w and x are shown in Fig. 1. The beam is supposed to have a mass per unit length m and a full plastic moment M_p, which may vary with temperature.

Then provided $\dot{\chi}_T$ is sufficiently small there will be a rigid phase of behaviour in which no plastic hinges develop. For higher values of $\dot{\chi}_T$ a discrete plastic hinge may be formed, and for still larger values there may be expanding and contracting hinges occupying varying lengths of the beam.

We suppose that the moving boundary of an expanding or contracting hinge occurs at $x = x_h$

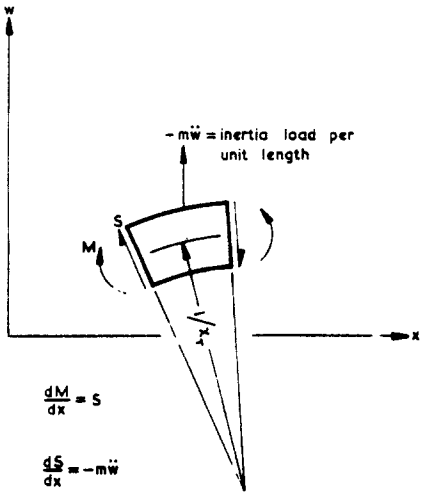

Fig. 1. Element of cantilever, showing sign conventions.

and that the hinge lies on the side $x < x_h$, so that for $x > x_h$ the beam is rigid. It is shown in Parkes[1] that within an expanding or contracting hinge the velocity $\dot{w}$ and thus the angular velocity $\dot{\theta}(= d\dot{w}/dx)$ at a given section is constant. We denote the section just within the hinge by the suffix h^- and that just outside it by h^+. At the boundary the slope of the beam is continuous but this is not necessarily true of the angular velocity. In fact it is shown in Parkes[1] that

$$(\dot{\theta})_{h^+} - (\dot{\theta})_{h^-} = \dot{\phi} \tag{1}$$

where $\dot{\phi}$ is zero during expansion but not during contraction. We now apply these ideas to the particular case of a cantilever of length l and in which x is measured from the root.

2.2 *The rigid cantilever*

For a cantilever in which the bending moment is everywhere less than M_p, we have

$$w = -\tfrac{1}{2}\chi_T x^2 + w_{pi} \tag{2}$$

where w_{pi} is the deflexion at the beginning of the regime due to some previous history of plastic deformation. By integration of the inertia loading we obtain

$$M = \frac{1}{24} m\ddot{\chi}_T (x^4 - 4l^3 x + 3l^4). \tag{3}$$

The bending moment is a maximum at the root ($x = 0$) and a plastic hinge will form there unless

$$-8M_p/ml^4 < \ddot{\chi}_T < 8M_p/ml^4 \tag{4}$$

2.3 *The cantilever with a hinge at the root*

If the condition of eqn (4) is violated, a plastic hinge will form at the root of the cantilever, producing a root slope due to the current regime of behaviour of θ_0. We then have

$$w = -\frac{1}{2}\chi_T x^2 + \theta_0 x + w_{pi}$$

$$S = m\left\{\frac{1}{6}\ddot{\chi}_T (x^3 - l^3) - \frac{1}{2}\ddot{\theta}_0 (x^2 - l^2)\right\}$$

and

$$M = m\left\{\frac{1}{24}\ddot{\chi}_T(x^4 - 4l^3x) - \frac{1}{6}\ddot{\theta}_0(x^3 - 3l^2x)\right\} + M_p$$

where we have made use of the conditions $S = 0$ at $x = l$ and $M = M_p$ at $x = 0$.

The further condition $M = 0$ at $x = l$ leads to

$$\ddot{\theta}_0 = \frac{3}{8}\ddot{\chi}_T l - \frac{3M_p}{ml^3}$$

and thus

$$S = \frac{m\ddot{\chi}_T}{48}(l - x)(l^2 - lx - 8x^2) - \frac{3}{2}\frac{M_p}{l^3}(l^2 - x^2) \tag{5}$$

and

$$M = \frac{m\ddot{\chi}_T}{48}x(l - x)^2(l + 2x) + \frac{M_p}{2l^3}(l - x)^2(2l + x). \tag{6}$$

Integrating the expression for $\ddot{\theta}_0$ and substituting back into that for the deflexion

$$w = -\frac{1}{2}\chi_T x^2 - \left[\frac{3}{ml^3}\int_{t_i}^{t}\int_{t_i}^{t} M_p \,\mathrm{d}t\,\mathrm{d}t + \frac{3}{8}l(\chi_{T_i} - \chi_T) + \left\{\frac{3}{8}l\dot{\chi}_{T_i} - \dot{\theta}_{o_i}\right\}(t - t_i)\right]x + w_{pi} \tag{7}$$

where the suffix i denotes the beginning of the regime and both $\dot{\theta}_{o_i}$ and w_{pi} are due to some previous plastic behaviour.

Differentiating (7) with respect to x and t and putting $x = 0$, we obtain the angular velocity at the root as

$$\dot{\theta}_o = \dot{\theta}_{o_i} + \frac{3}{8}l(\dot{\chi}_T - \dot{\chi}_{T_i}) - \frac{3}{ml^3}\int_{t_i}^{t} M_p \,\mathrm{d}t. \tag{8}$$

It will be noted that the shear force (eqn 5) is zero when $x = l$ and when $l^2 + lx - 8x^2 = \gamma l(l + x)$ where $\gamma = 72M_p/m\ddot{\chi}_T l^4$. The quadratic equation leads to $x/l = \frac{1}{16}(1 - \gamma + \beta)$ where $\beta = \{(1 - \gamma)(33 - \gamma)\}^{1/2}$. Substituting in eqn (5) we then find

$$M = \frac{M_p}{32768\gamma}\{63 + 66\gamma - \gamma^2 + (15 + \gamma)\beta\}(15 + \gamma - \beta)^2.$$

This is a maximum value of the bending moment and we have to compare it with $\pm M_p$. For $M = +M_p$, $\gamma = 1$ and $x/l = 0$. For $M = -M_p$, $\gamma = -0.286$ and $x/l = 0.489$ with $\ddot{\chi}_T = -252\,M_p/ml^4$. Plasticity will occur other than at the root hinge unless

$$-252M_p/ml^4 < \ddot{\chi}_T \leqslant 72M_p/ml^4. \tag{9}$$

The corresponding conditions when $M = -M_p$ at $x = 0$ are

$$-72\,M_p/ml^4 \leqslant \ddot{\chi}_T < 252M_p/ml^4.$$

2.4 *The cantilever with an extensive hinge*

The general theory of expanding and contracting hinges was developed in Parkes [1], and the analysis of Section 2.3 of that paper can be adopted *in toto*. In particular it was shown that during the expansion phase of a hinge extending from $x = 0$ to x_h,

$$(\dot{\theta})_{h^-} = \left(\frac{72M_p}{m}\right)^{1/4}\left[\dot{\chi}_T\ddot{\chi}_T^{-(1/4)} - \frac{2}{3}\int(\ddot{\chi}_T)^{3/4}\,\mathrm{d}t\right]_{t_i}^{t} + (\dot{\theta})_{h_i}. \tag{10}$$

Since $\dot{\theta}$ at a given value of x within the hinge is constant, eqn (10) gives the distribution of angular velocity within the hinge provided that t is replaced by t_x, the time at which section x entered the hinge, and the final term is replaced by $\dot{\theta}_i$, the angular velocity at x at the beginning of the regime ($t = t_i$).

Equation (10) can be integrated to give the velocity within the expanding hinge ($0 < x \leqslant x_h$) as

$$\dot{w} = \left(\frac{72M_p}{m}\right)^{1/4} \int_0^x \left[\dot{\chi}_T \ddot{\chi}_T^{-(1/4)} - \frac{2}{3}\int (\ddot{\chi}_T)^{3/4}\,dt\right]_{t_i}^{t_x} + \int_0^x \dot{\theta}_i\,dx. \tag{11}$$

Since, in the expansion phase, the angular velocity is continuous at $x = x_h$, the velocity outside the hinge ($x_h \leqslant x \leqslant l$) is given by

$$\dot{w} = (\dot{w})_h + (\dot{\theta})_{h-}(x - x_h) - \frac{1}{2}\dot{\chi}_T(x - x_h)^2. \tag{12}$$

where $(\dot{w})_h$ and $(\dot{\theta})_{h-}$ are obtained from eqns (11) and (10). Equations (11) and (12) can be integrated with respect to time in order to obtain deflexions.

For a contracting hinge which has previously expanded through a particular value of x, the velocity within the hinge during contraction has the same value as during the expansion. The velocities outside the hinge during contraction differ from those during expansion because of the discontinuity in angular velocity at $x = x_h$. From Parkes [1] we have that this discontinuity is given by

$$\dot{\phi} = \frac{1}{3}(\dot{\chi}_{T_c} - \dot{\chi}_{T_e})(l - x_h) \tag{13}$$

where

$$l - x_h = \left[\frac{72\int_{t_e}^{t_c} M_p\,dt}{m(\dot{\chi}_{T_c} - \dot{\chi}_{T_e})}\right]^{1/4} \tag{14}$$

and the suffices e and c refer to expansion and contraction respectively. Equation (12) is replaced by

$$\dot{w} = (\dot{w})_h + \{(\dot{\theta})_{h-} + \dot{\phi}\}(x - x_h) - \frac{1}{2}\dot{\chi}_T(x - x_h)^2. \tag{15}$$

For the case of the cantilever we shall be particularly concerned with a hinge phenomenon which was mentioned only very briefly in the earlier paper: the hinge which is created instantaneously at its maximum extent, and then contracts, there being no expansion phase. Suppose that this hinge is created at time $t = t_i$ when $d\dot{\theta}/dx$ is equal to $-\dot{\chi}_{T_i}$. Let the hinge extend initially from $x = 0$ to x_{h_i} and let it then contract to $x_h (< x_{h_i})$. Since x_h is a section within the hinge, the velocity $(\dot{w})_h$ remains constant during the contraction, as does the angular velocity $(d\dot{\theta}/dx)_{h-}$ at the value $-\dot{\chi}_{T_i}$.

Then the initial momentum (at $t = t_i$) of the part of the cantilever between $x = x_h$ and l is

$$m(l - x_h)(\dot{w})_h - m\int_{x_h}^{l}\int_{x_h}^{x}\int_{x_h}^{x} \dot{\chi}_{T_i}\,dx\,dx\,dx$$

and the momentum when the hinge has contracted to x_h is

$$m(l - x_h)(\dot{w})_h - m\int_{x_h}^{l}\int_{x_h}^{x}\int_{x_h}^{x} \dot{\chi}_T\,dx\,dx\,dx + \tfrac{1}{2}m(l - x_h)^2\dot{\phi}.$$

Since x_h is within the hinge, where the bending moment is everywhere M_p and the shear force

is zero, we may equate these and obtain

$$\dot{\phi} = \frac{1}{3}(\dot{\chi}_T - \dot{\chi}_{T_i})(l - x_h). \tag{16}$$

The initial angular momentum of the part of the cantilever between $x = x_h$ and l, about x_h, is

$$\frac{1}{2}m(l - x_h)^2(\dot{w})_h - m\int_{x_h}^{l}(x - x_h)\int_{x_h}^{x}\int_{x_h}^{x}\dot{\chi}_{T_i}\,dx\,dx\,dx$$

and the angular momentum when the hinge has contracted to x_h is

$$\frac{1}{2}m(l - x_h)^2(\dot{w})_h - m\int_{x_h}^{l}(x - x_h)\int_{x_h}^{x}\int_{x_h}^{x}\dot{\chi}_T\,dx\,dx\,dx + \frac{1}{3}m(l - x_h)^3\dot{\phi}.$$

Equating the difference of these to the angular impulse imparted by the hinge at x_h, and substituting for $\dot{\phi}$ from eqn (16), we find

$$l - x_h = \left[\frac{72\int_{t_i}^{t} M_p\,dt}{m(\dot{\chi}_T - \dot{\chi}_{T_i})}\right]^{1/4}. \tag{17}$$

For the hinge which is created instantaneously and then contracts, eqns (16) and (17) replace (13) and (14). If the instantaneously created hinge expands before contraction, eqns (13) and (14) are used until the hinge has regained its original length, and then eqns (16) and (17) are employed for the further contraction, the time t_i being taken as that of the initial creation. It may be noted that eqns (16) and (17) can alternatively be obtained by integration of eqns (16) and (17) of Parkes[1], using appropriate initial conditions.

3. ZONES OF BEHAVIOUR IN THE CANTILEVER SUBJECTED TO A SINUSOIDAL HEATING PULSE

We now apply the theory of the previous section to the case of a cantilever subjected to a variation of thermal curvature such that

$$\left.\begin{aligned} \chi_T &= (AM_p/\omega^2 ml^4)(\omega t - \sin\omega t) \quad \text{for} \quad 0 \leqslant \omega t \leqslant 2\pi \\ \text{and} \qquad \chi_T &= 2\pi AM_p/\omega^2 ml^4 \quad \text{for} \quad \omega t \geqslant 2\pi \end{aligned}\right\} \tag{18}$$

where A is a dimensionless parameter determining the rapidity of heating, $2\pi/\omega$ is the period of the heating pulse, and M_p is taken as independent of temperature. This temporal variation is characteristic of neutron heating in a pulsed reactor[21]. Laser heating may tend more to a skew triangular form for $\dot{\chi}_T$[22], but the behaviour of the cantilever is unlikely to be very sensitive to pulse shape[8].

From eqn (4) it will be seen that the cantilever remains rigid provided that $A \leqslant 8$. For $A > 8$ a hinge forms at the root at time t_1 when

$$\omega t_1 = \arcsin(8/A). \tag{19}$$

The angular velocity of the root hinge is given by eqn (8), with $\dot{\theta}_{o_i} = 0$. Provided that $A < 72$ (eqn 9) this angular velocity returns to zero at time t_2 when

$$\cos\omega t_1 - \cos\omega t_2 = (\omega t_2 - \omega t_1)\sin\omega t_1. \tag{20a}$$

If the root hinge is to be followed by a further rigid phase, ωt_2 must be less than $\omega t_1 + \pi$. From (19) and (20a), A must then be less than $4(4 + \pi^2)^{1/2} = 14.9$.

For $A < 14.9$, the root hinge is followed by a rigid cantilever regime until $\omega t_1 + \pi$, when a

negative root hinge is formed ($M = -M_p$). For $A > 14.9$, the negative root hinge follows directly after the positive hinge rotation has ceased. The analysis of the negative root hinge is similar to that for the positive root hinge, except for the change from $+M_p$ to $-M_p$. From eqns (8), (19) and (20a) the negative hinge rotation ceases at t_3, where

$$\left.\begin{array}{ll} \omega t_3 = \omega t_2 + \pi & (8 < A < 11.0) \\ \omega t_3 = \omega t_1 + \pi + (1 + \cos \omega t_1)/\sin \omega t_1 & (11.0 < A < 14.9) \\ \omega t_3 = \omega t_2 + (1 - \cos \omega t_2)/\sin \omega t_1 & (14.9 < A < 72)\dagger. \end{array}\right\} \tag{21a}$$

The boundary at $A = 11.0$ corresponds to $\omega t_3 = 2\pi$.

For $A > 72$, the positive root hinge is followed by an expanding hinge at time t_4 when

$$\omega t_4 = \arcsin (72/A). \tag{22}$$

The hinge extends from $x = 0$ to x_h, where according to Parkes[1]

$$x_h = l - (72M_p/m\ddot{\chi}_T)^{1/4}. \tag{23}$$

It reaches its maximum size when $\omega t = \pi/2$. The contraction phase is described by eqn (14). From this equation and (22), contraction ends ($x_h = 0$) at t_5 where

$$\cos \omega t_4 - \cos \omega t_5 = (\omega t_5 - \omega t_4) \sin \omega t_4. \tag{24}$$

The ensuing positive root hinge persists until its angular velocity returns to zero at time t_2, where we shall show that this is the same time as that given by eqn (20a). From eqn (8),

$$\begin{aligned} 0 &= \dot{\theta}_{o_5} + \frac{3}{8} l(\dot{\chi}_{T_2} - \dot{\chi}_{T_5}) - (3M_p/ml^3)(t_2 - t_5) \\ &= \dot{\theta}_{o_4} + \dot{\phi}_5 + \frac{3}{8} l(\dot{\chi}_{T_2} - \dot{\chi}_{T_5}) - (3M_p/ml^3)(t_2 - t_5). \end{aligned}$$

Using (8) to give $\dot{\theta}_{o_4}$ and (13) to give $\dot{\phi}_5$, we obtain on substituting from (22) and (24) that

$$\cos \omega t_1 - \cos \omega t_2 = (\omega t_2 - \omega t_1) \sin \omega t_1. \tag{20b}$$

The solutions of eqns (20) or (24) are clearly of importance in defining the zones of behaviour of the cantilever. It is worth noting that for small values of ωt_1,

$$\omega t_2 = 2\pi - \{4\pi\omega t_1 - 4\pi^{1/2}(\omega t_1)^{3/2} + (\tfrac{4}{3}\pi^2 - 1)(\omega t_1)^2\}^{1/2}.$$

Up to this point, the analysis of the rapidly heated cantilever has displayed modes of behaviour very similar to those shown for the free beam in Parkes[1]. After the cessation of positive hinge rotation at time t_2, however, the behaviour of the cantilever (for $A > 72$) is very different from that of the free beam. The essential reason for this different behaviour is that for the cantilever, for $A > 72$, all values of ωt_2 exceed $3\pi/2$.

For $72 < A < 83.2$, the positive root hinge is followed by a negative root hinge which persists until time t_3 given by the last of eqns (21), after which all motion ceases. We thus have a type of behaviour between $A = 72$ and 83.2 in which a positive expanding and contracting hinge is not followed by a corresponding negative expanding and contracting hinge: this omission is not found in the free beam.

For $A > 83.2$, the positive root hinge is followed by the instantaneous creation of a negative hinge of finite extent, which subsequently contracts to a simple root hinge at time t_6. The governing equation of the motion is (17), and on substituting an initial time of t_2 and noting that

†It is shown subsequently that the condition $A < 72$ may be relaxed.

M_p is to be taken as negative we obtain with $x_h = 0$ and by using eqn (19)

$$\cos \omega t_2 - \cos \omega t_6 = (\omega t_2 - \omega t_6) \sin \omega t_1. \tag{25}$$

After time t_6 there is a negative root hinge. Since the angular velocity of the root hinge was zero at time t_2, its velocity at time t_6 is given simply by $\dot{\theta}_{o_6} = \dot{\phi}_{o_6}$, which from eqn (16) with $x_h = 0$ and M_p negative leads to

$$\dot{\theta}_{o_6} = \frac{1}{3}(\cos \omega t_2 - \cos \omega t_6) A M_p / \omega m l^3.$$

Rotation ceases, from eqn (8), at time t_3 when

$$0 = \dot{\theta}_{o_6} + \frac{3}{8}(\cos \omega t_6 - 1)(A M_p / \omega m l^3) + 3(\omega t_3 - \omega t_6)(M_p / \omega m l^3).$$

Substituting for $\dot{\theta}_{o_6}$ from the previous equation, and using eqns (19) and (25),

$$\omega t_3 = \omega t_2 + (1 - \cos \omega t_2)/\sin \omega t_1. \tag{21b}$$

It will be noted that eqn (21b) is identical with the last of eqns (21a) and that hinge spreading has no effect on the time t_3 at which motion finally ceases.

The zones of behavior of the cantilever defined by eqns (19), (20a, b), (21a, b), (22), (24) and (25) are plotted as functions of A and ωt in Fig. 2. The extent of the hinges is defined by contours of $h(= x_h/l)$ obtained from eqns (23), (14) and (17).

4. ACCELERATIONS, VELOCITIES AND DISPLACEMENTS FOR $A = 200$

4.1 *Zones of behaviour*

In our analysis so far, and in Parkes[1], although zones of behaviour have been determined, no attempt has been made to study the details of the motions. As an example, we now propose to do this for the cantilever subjected to a sinusoidal heating pulse of the type defined by eqn (18) and with $A = 200$ (i.e. a heating rate 25 times greater than that at which plasticity is first produced). The zones of behaviour are shown at the uppermost limit of Fig. 2: their boundaries are at $\omega t_1 = 0.040$, $\omega t_4 = 0.368$, $\omega t_5 = 4.225$, $\omega t_2 = 5.601$, $\omega t_6 = 6.216$ and $\omega t_3 = 11.19$.

4.2 *Accelerations*

For $0 < \omega t \leq 0.040$ the cantilever remains rigid and the acceleration is given from eqns (2) and (18), with $A = 200$, in the non-dimensional form

$$\ddot{w} m l^2 / M_p = -100 \sin \omega t (x^2/l^2). \tag{26}$$

For $0.040 < \omega t \leq 0.368$ there is a positive root hinge and from eqn (7), with appropriate substitutions,

$$\ddot{w} m l^2 / M_p = -100 \sin \omega t (x^2/l^2) + (75 \sin \omega t - 3)(x/l). \tag{27}$$

For $0.368 < \omega t \leq \pi/2$ there is an expanding positive hinge. For sections of the cantilever outside the hinge ($h < x/l \leq 1$) the acceleration is given by eqn (13) of Parkes[1] as

$$\ddot{w} m l^2 / M_p = -100 \sin \omega t \left(\frac{x}{l} - h\right)^2 + \frac{24}{(1-h)^3}\left(\frac{x}{l} - h\right) \tag{28}$$

where we have made use of the relationship for expansion (eqn 23)

$$h = 1 - (72/A \sin \omega t)^{1/4}.$$

The acceleration within the hinge is, of course, zero.

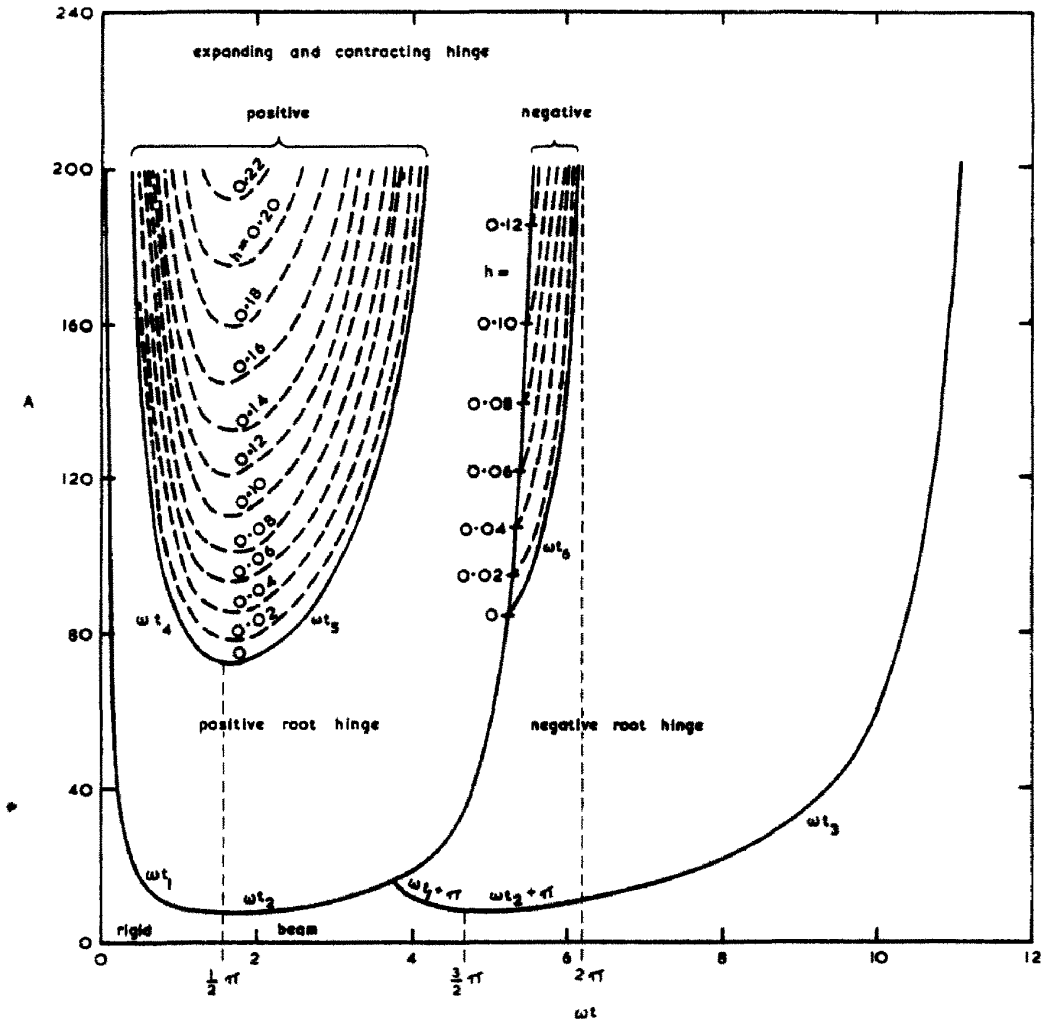

Fig. 2. Zones of behaviour.

The hinge reaches its maximum extent, $h = 0.2254$, at $\omega t = \pi/2$, and for $\pi/2 < \omega t \leqslant 4.225$ the hinge contracts. The acceleration outside the hinge can again be obtained from eqn (13) of Parkes[1] as

$$\ddot{w}ml^2/M_p = -100 \sin \omega t \left(\frac{x}{l} - h\right)^2 + \left\{100 \sin \omega t(1-h) - \frac{12}{(1-h)^3}\right\}\left(\frac{x}{l} - h\right) + \frac{6}{(1-h)^2} - \frac{100}{6} \sin \omega t(1-h)^2 \quad (29)$$

where h is determined by eqn (14) during contraction.

For $4.225 < \omega t \leqslant 5.601$ there is a positive root hinge and eqn (27) again applies.

For $5.601 < \omega t \leqslant 6.216$ there is a negative contracting hinge. The equation for the acceleration outside the hinge is similar to (29) except that terms derived from M_p change sign. We have

$$\ddot{w}ml^2/M_p = -100 \sin \omega t \left(\frac{x}{l} - h\right)^2 + \left\{100 \sin \omega t(1-h) + \frac{12}{(1-h)^3}\right\}\left(\frac{x}{l} - h\right) - \frac{6}{(1-h)^2} - \frac{100}{6} \sin \omega t(1-h)^2. \quad (30)$$

For $6.216 < \omega t \leqslant 2\pi$ there is a negative root hinge and we have an equation for the

acceleration similar to (27), but again with the sign of the M_p term reversed. Thus

$$\ddot{w}ml^2/M_p = -100 \sin \omega t \left(\frac{x}{l} - h\right)^2 + (75 \sin \omega t + 3)(x/l). \tag{31}$$

For $2\pi < \omega t \leqslant 11.19$ the negative root hinge continues, but because of the constant thermal curvature (eqn 18),

$$\ddot{w}ml^2/M_p = 3(x/l). \tag{32}$$

At $\omega t = 11.19$ motion ceases.

The accelerations given by eqns (26)–(32) are plotted in Figs. 3 for $x/l = 0.04$, 0.08, 0.12, 0.16, 0.20 and 1.00. For each of the sections up to $x/l = 0.20$ there is an initial increasing positive acceleration through the rigid beam and root hinge phases which diminishes to zero again as the section enters the expanding hinge (the hinge has a maximum extent of $h = 0.2254$). There is a period of zero acceleration while the section lies within the hinge which is terminated by a sudden discontinuity to a new positive acceleration as the section leaves the contracting hinge. When contraction ceases at $\omega t = 4.225$ there is another discontinuity to a negative acceleration accompanying a further root hinge phase. This ends at $\omega t = 5.601$ with the instantaneous creation of a negative contracting hinge of extent $h = 0.1303$. The accelerations at sections $x/l = 0.04$, 0.08 and 0.12, being within the hinge, immediately become zero, but those at $x/l = 0.16$ and 0.20, being outside the hinge, change to non-zero values. The accelerations at $x/l = 0.04$, 0.08 and 0.12 jump to new negative values as each section leaves the contracting hinge. Contraction ceases at $\omega t = 6.216$ and there are discontinuous changes in all accelerations as the negative root hinge phase begins. For $\omega t > 2\pi$ the accelerations become constant until motion ceases at $\omega t = 11.19$. The accelerations for $x/l = 1.00$ are typical of those for sections remote from the hinges, with discontinuities at $\omega t = 4.225$, 5.601 and 6.216.

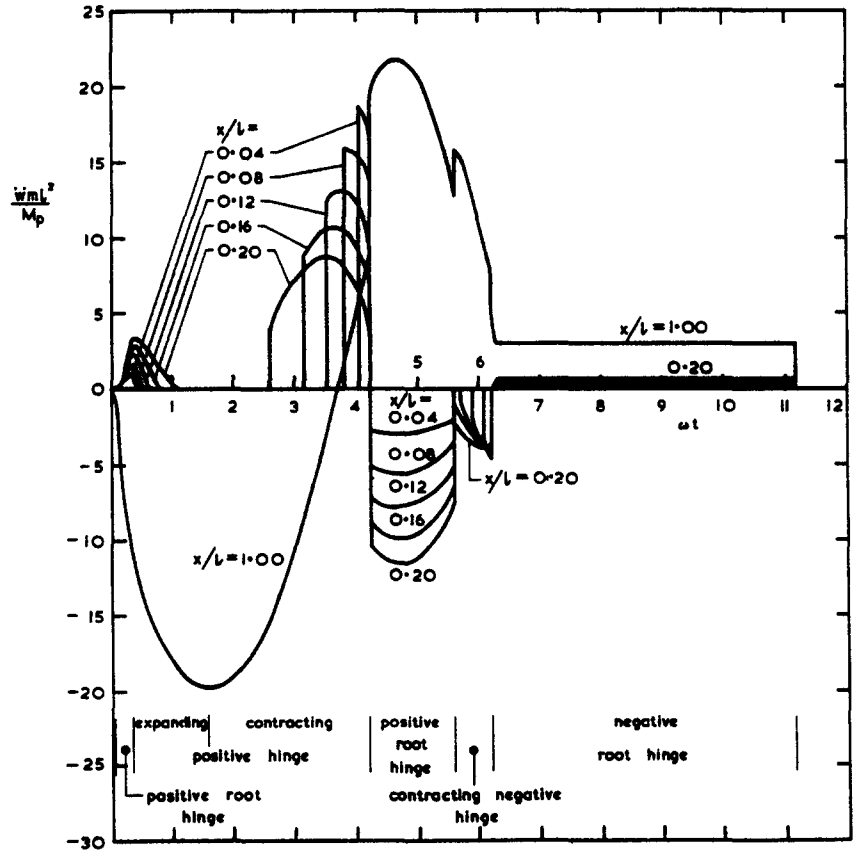

Fig. 3. Accelerations for $A = 200$.

4.3 *Velocities*

The velocities of the cantilever are conveniently expressed in the non-dimensional form $\dot{w}ml^2\omega/M_p$. They can be obtained by numerical integration of Fig. 3 or in some cases by direct calculation. The velocities at sections $x/l = 0.04$, 0.08, 0.12, 0.16 and 0.20 are shown in Fig. 4. The broken lines indicate the boundaries of the zones of constant velocity when the sections concerned are within expanding or contracting hinges.

4.4 *Displacements*

The displacements of the cantilever, expressed non-dimensionally as $wml^2\omega^2/M_p$, can be obtained by integration of Fig. 4 or in some cases by direct calculation. After motion has ceased ($\omega t > 11.19$) we have a final displacement which includes the thermal curvature χ_T. This curvature will eventually be relieved by thermal conduction. Assuming that the attainment of isothermal conditions is not accompanied by further plastic deformation we may subtract a displacement of $-\frac{1}{2}\chi_T x^2$. The final displacements before and after the relief of thermal curvature are plotted in Fig. 5. It will be noted that after the relief of thermal curvature that part of the cantilever between $x/l = 0.2254$ and 1 is straight, since it has not been subjected to plastic deformation, whereas the part between $x/l = 0$ and 0.2254 shows a permanent curvature which is the result of the positive expanding and contracting hinge, combined, for $x/l < 0.1303$, with the effect of the negative contracting hinge. The value of $wml^2\omega^3/M_p$ at the tip is 402.9 and the slope of the outer portion 453.3. The root hinge angle is quite small at 42.3, so that more than 90% of the deformation takes place in the extensive hinges.

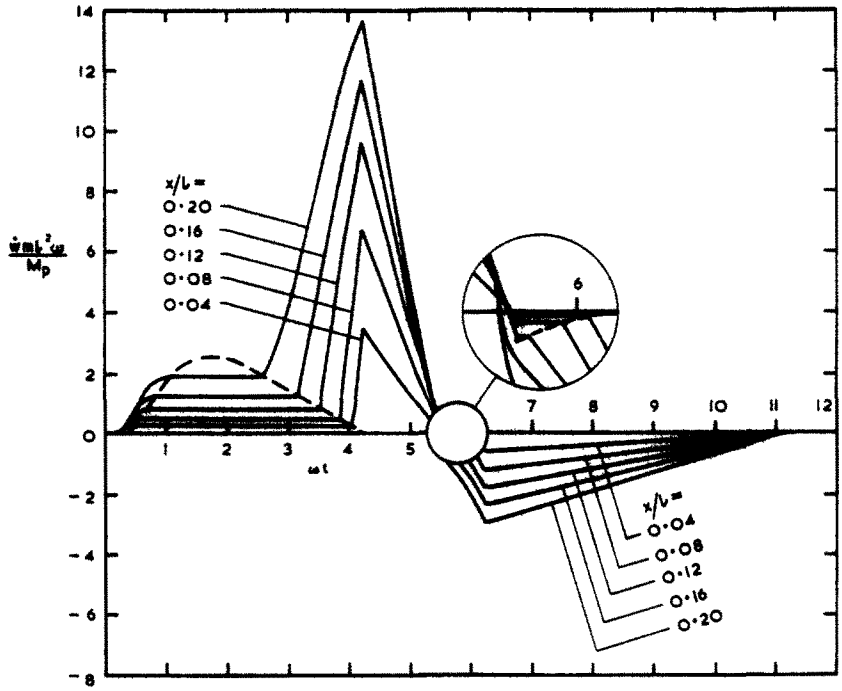

Fig. 4. Velocities for $A = 200$.

5. THE STRONG BEAM

The behaviour of a cantilever subjected to very rapid thermal curvature is complicated and extensive calculation is needed to predict the final deformation. It seems reasonable to seek for some simplifying assumption which may lead to sufficiently accurate predictions with less labour. One possibility is to restrict deformation to a root hinge and to assume that the sectional properties of the rest of the cantilever are sufficiently strong so that it does not deform plastically even though the bending moment exceeds M_p. Under these circumstances there will be an initial rigid phase followed at time t_1 by a positive root hinge. This will end at time t_2 and will be followed by a negative root hinge which will continue until motion ceases at time t_3. We

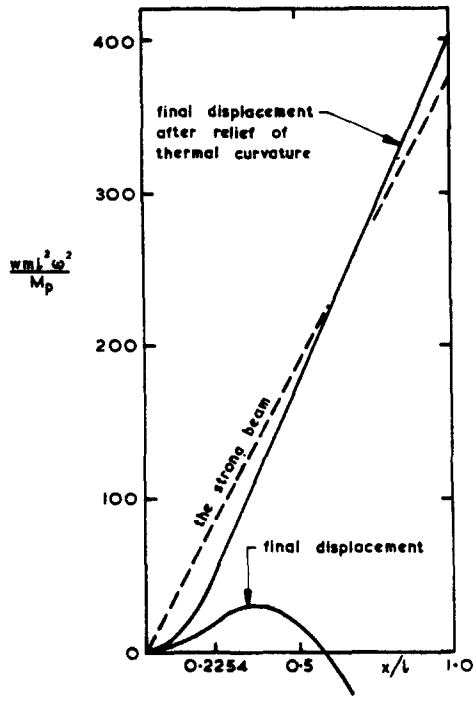

Fig. 5. Final displacements for $A = 200$.

have already shown in Section 3 that the values of t_2 are not affected by hinge spreading. The times t_1, t_2 and t_3 will thus still be given by eqns (19), (20b) and (21b).

The rotation of the root hinge can be found by differentiating eqn (7) with respect to x and putting $x = 0$. For the positive phase we have

$$\theta_{o_2} = \frac{3}{8} l \{\chi_{T_2} - \chi_{T_1} - \dot{\chi}_{T_1}(t_2 - t_1)\} - \frac{3}{2}\frac{M_p}{ml^3}(t_2 - t_1)^2,$$

and for the negative phase

$$\theta_{o_3} - \theta_{o_2} = \frac{3}{8} l \{\chi_{T_3} - \chi_{T_2} - \dot{\chi}_{T_2}(t_3 - t_2)\} + \frac{3}{2}\frac{M_p}{ml^3}(t_3 - t_2)^2.$$

Adding the two equations and substituting for the thermal curvature and times, we finally obtain the non-dimensional root hinge rotation for $A = 200$ as $\theta_{o_3} ml^3\omega^2/M_p = 378.1$.

After the relief of thermal curvature we thus have a straight cantilever of slope 378.1. This is shown by the broken line in Fig. 5. The tip deflection $wml^2\omega^2/M_p = 378.1$ is some 6% less than the true value of 402.9 obtained when plastic deformation spreads over nearly a quarter of the length of the cantilever.

6. RANGE OF VALIDITY OF THE ANALYSIS

6.1 *Longitudinal inertia effects*

Since rapid thermal curvature can only be produced by heating, and not by cooling, it is impossible for the thermal curvature to be accompanied by zero net longitudinal strain, as occurs in most other forms of impulsive loading. It follows that the cantilever subjected to rapid thermal curvature will tend to expand, and longitudinal inertia forces will be induced. For neutron or radiation heating the thermal strain ϵ_T will commonly vary exponentially with the depth, so that for a rectangular section of depth d we may put

$$\epsilon_T = K e^{(2\lambda/d)y} \tag{33}$$

where K is a time-dependent function, λ is a constant and y is a co-ordinate measured from the centre of the section towards the heat source. We then have

$$\chi_T = \frac{12}{d^3}\int_{-(1/2)d}^{(1/2)d} \epsilon_T y \, dy = \frac{6K}{d\lambda^2}(\lambda \cosh \lambda - \sinh \lambda)$$

$$\epsilon_{T_{av}} = \frac{1}{d}\int_{-(1/2)d}^{(1/2)d} \epsilon_T \, dy = \frac{K}{\lambda}\sinh \lambda$$

$$\epsilon_{T_{max}} = K e^{\lambda}$$

where the suffices av and max stand for average and maximum values. Thus

$$\chi_T d = 6\left(\coth \lambda - \frac{1}{\lambda}\right)\epsilon_{T_{av}} \tag{34}$$

$$\epsilon_{T_{max}} = \lambda e^{\lambda} \operatorname{cosech} \lambda \epsilon_{T_{av}}. \tag{35}$$

For a beam which absorbs most of the incident radiation, which is a prerequisite for bending phenomena to occur, λ is unlikely to be less than 0.5. There is an upper limit set by eqn (35) if $\epsilon_{T_{av}}$ is to produce significant longitudinal forces and the outer surface is not to melt: this upper limit will vary with the material but may be at about $\lambda = 20$.

We shall assume that up to the time of yielding we may use the analysis of Parkes and Carter [21] where the longitudinal force P in a uniform rod held at one end and subjected to a thermal strain $\epsilon_{T_{av}}$ is given by $FE\epsilon_{T_{av}}bd$ where E is the Young modulus, b is the breadth of the section and F is a stress factor dependent on the parameter $B = (\omega l/2\pi)(\rho/E)^{1/2}$ where ρ is the density of the material.

Putting the full plastic force as $P_p = \sigma_y bd$ where σ_y is the yield stress we have

$$\frac{P}{P_p} = \frac{FE\epsilon_{T_{av}}}{\sigma_y}.$$

Yielding of the rigid-plastic cantilever in bending first occurs at the root (see Fig. 2) at a time not later than $\omega t = \pi/2$. Substituting in the above equation from eqn (34), from the first of eqns (18) with $\omega t = \pi/2$ and putting $M_p = \sigma_y bd^2/4$ and $m = \rho bd$ we have on utilising the equation for B,

$$\frac{P}{P_p} < \frac{A\left(\frac{\pi}{2} - 1\right)}{96\pi^2\left(\coth \lambda - \frac{1}{\lambda}\right)}\frac{F}{B^2}\frac{d^2}{l^2} \tag{36}$$

where the inequality occurs because in taking the first of eqns (18) with $\omega t = \pi/2$ we have overestimated the value of χ_T.

Since yielding first occurs at the root we need the value of $[F]_{x=0}$. This is given from eqn (23) of Parkes and Carter [21] as

$$[F]_{x=0} = \left| \sum_{n=1,3,5} \frac{256B^3}{\pi^2 n^2(1 - 16B^2)} \frac{\sin(n\pi/4B)}{\sin \frac{1}{2}n\pi} \right|.$$

This is the peak value of the stress factor and it will not necessarily co-incide in time with the onset of bending yielding.

It is a characteristic of rigid-plastic theory that we assume E to be very large. It follows that B will be small. For small values of B, the above equation for $[F]_{x=0}$ can be represented with sufficient accuracy by taking the first term only and by ignoring $16B^2$ compared with unity. We shall take what will generally be a high value for the stress factor by writing the term $\sin(\pi/4B)$

as unity. We then have

$$[F]_{x=0} = \frac{256B^3}{\pi^2}. \tag{37}$$

Substituting eqn (37) in (36) we obtain

$$\frac{P}{P_p} < \frac{256\left(\frac{\pi}{2}-1\right)AB}{96\pi^4\left(\coth\lambda - \frac{1}{\lambda}\right)}\frac{d^2}{l^2}. \tag{38}$$

From this point onwards it will be convenient if we retain the length l of the cantilever only in the length-to-depth ratio

$$\mu = l/d \tag{39}$$

and eliminate it from the other non-dimensional parameters. Instead of A and B we shall therefore use

$$\left.\begin{aligned} \kappa &= \dot{A}/B^2\mu^2 = 8\pi\chi_{T_{max}}d(E/\sigma_y) \\ \text{and} \\ \Omega &= B/\mu = \frac{1}{2\pi}\omega d(\rho/E)^{1/2} \end{aligned}\right\} \tag{40}$$

Equation (38) then becomes

$$\frac{P}{P_p} < \frac{256\left(\frac{\pi}{2}-1\right)\kappa\Omega^3\mu^3}{96\pi^4\left(\coth\lambda - \frac{1}{\lambda}\right)}. \tag{41}$$

Remembering that the yield equation is $(P/P_p)^2 + (M/M_p) = 1$, the fractional change in the yield moment due to the presence of the longitudinal force is less than the square of the r.h.s. of inequality (41). This expression is not very sensitive to changes in λ and so we shall take λ as large and thus $\{\coth\lambda - (1/\lambda)\}$ equal to unity. We then have

$$\text{Fractional error in } M_p < 2.44 \times 10^{-4}\kappa^2\Omega^6\mu^6. \tag{42}$$

An alternative way in which longitudinal forces might contribute to errors in M_p would be if deflexions became sufficiently large for the product of end thrust and deflexion to form a significant fraction of the full plastic moment. Up to first yield, the thermal deflexion $\chi_T x^2/2$ represents the true deflexion. After yielding, it substantially overestimates the deflexions. The longitudinal force at the free end of the cantilever must be zero, but from Parkes and Carter [21] it seems that a constant force may persist from the root up to about $x/l = 0.8$. Multiplying the longitudinal force by the deflexion, we obtain a contribution to the bending moment of $FE\epsilon_{T_{av}}bd\chi_T(0.8l)^2/2$. Substituting from eqn (34) for $\epsilon_{T_{av}}$ and from (37) for F, and choosing the value of χ_T from the first of eqns (18) with $\omega t = \pi/2$, we find on making the substitutions of eqns (39) and (40) that the contribution to the bending moment can be expressed for λ large as

$$\text{Fractional error in } M_p < 7.23 \times 10^{-5}\kappa^2\Omega^3\mu^5(\sigma_y/E) \tag{43}$$

where the inequality arises from the overestimates of deflexion and of stress factor. It will be noted that inequality (43) retains an additional non-dimensional parameter (σ_y/E).

6.2 *Elastic effects*

As with all rigid-plastic analysis, the work in the present paper can only be applied to real materials provided that the elastic deformations are small compared with those due to plastic

flow. In the present case this means that the maximum possible elastic strain σ_y/E must be small compared with the maximum thermal strain $\epsilon_{T_{max}}$ which is also a measure of the final plastic strain. We thus have

$$\text{Fractional error in final plastic strain} = \sigma_y/E\epsilon_{T_{max}} \tag{44}$$

or, using (34), (35) and first of eqns (40),

$$\text{Fractional error in final plastic strain} = \frac{48\pi}{\kappa}\left\{\frac{\left(\coth\lambda - \frac{1}{\lambda}\right)}{\lambda\, e^{\lambda}\, \operatorname{cosech}\lambda}\right\}.$$

The term in λ has a maximum value at $\lambda = 1.35$ of 0.139, whence

$$\text{Fractional error in final plastic strain} < 21/\kappa. \tag{45}$$

It may be noted that for $0.5 < \lambda < 4$, the ratio of the maximum possible elastic curvature to the maximum thermal curvature is about three times the fractional error in the final plastic strain.

6.3 *Limitations*

The zones of values of Ω and κ for which the errors in M_p and in the final plastic strain are less than 10% or 5% are plotted in Fig. 6 for $\mu = 10$, 50 and 250 and $E/\sigma_y = 1000$. It may be noted that inequality (42) is of significance for $\mu = 10$ only. The important inequalities are (43) and (45).

The author has been subjecting small shim steel specimens, 10 mm long by 0.06 mm deep to laser heating of about 300μs duration. Allowance has to be made for conduction in these thin specimens and as a result the effective value of λ is about $\frac{1}{2}$. With a front face temperature of 1000°C, the non-dimensional parameters are $\mu = 167$, $\Omega = 5 \times 10^{-5}$ and $\kappa = 350$, so that the worst

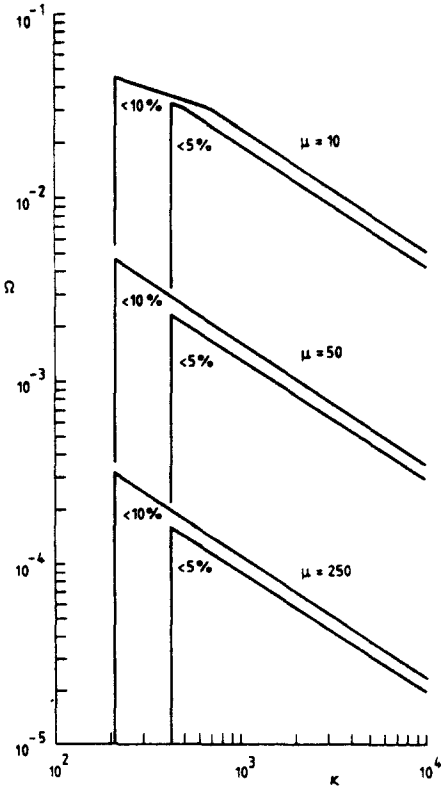

Fig. 6. Values of μ, Ω and κ for which errors defined by eqns (42), (43) and (45) are less than 10% or less than 5%. $E/\sigma_y = 1000$.

error is in the hypothesis of rigidity: in fact the maximum elastic strain is about 5% of the maximum thermal strain. Longitudinal inertia effects are quite unimportant.

REFERENCES

1. E. W. Parkes, The expanding and contracting hinge in a rapidly heated rigid-plastic beam. *Proc. R. Soc. Lond.* **A337**, 351–364 (1974).
2. J. F. Baker, Plasticity as a factor in the design of war-time structures. In *The Civil Engineer in War*, Vol. 3, 30–51. The Institution of Civil Engineers, London (1948).
3. P. E. Duwez, D. S. Clark and H. F. Bohnenblust, The behaviour of long beams under impact loading. *J. Appl. Mech.* **17**, 27–34 (1950).
4. M. F. Conroy, Plastic-rigid analysis of long beams under transverse impact loading. *J. Appl. Mech.* **19**, 465–470 (1952).
5. E. W. Parkes, Some simple experiments on the dynamic plastic behaviour of mild-steel beams. *Brit. Weld. J.* **3**, 362–366 (1956).
6. E. W. Parkes, The permanent deformation of an encastré beam struck transversely at any point in its span. *Proc. Inst. Civ. Engrs.* **10**, 277–304 (1958).
7. E. H. Lee and P. S. Symonds, Large plastic deformations of beams under transverse impact. *J. Appl. Mech.* **19**, 308–314 (1952).
8. P. S. Symonds, Dynamic load characteristics in plastic bending of beams. *J. Appl. Mech.* **20**, 475–481 (1953).
9. P. S. Symonds and C. F. A. Leth, Impact of finite beams of ductile metal. *J. Mech. Phys. Solids* **2**, 92–102 (1954).
10. E. W. Parkes, The permanent deformation of a cantilever struck transversely at its tip. *Proc. R. Soc. Lond.* **A228**, 462–476 (1955).
11. T. J. Mentel, The plastic deformation due to impact of a cantilever beam with an attached tip mass. *J. Appl. Mech.* **25**, 515–524 (1958).
12. S. R. Bodner and P. S. Symonds, Experimental and theoretical investigation of the plastic deformation of cantilever beams subjected to impulsive loading. *J. Appl. Mech.* **29**, 719–728 (1962).
13. S. R. Bodner and W. G. Speirs, Dynamic plasticity experiments on aluminium cantilever beams at elevated temperatures. *J. Mech. Phys. Solids* **11**, 65–77 (1963).
14. T. C. T. Ting, The plastic deformation of a cantilever beam with strain-rate sensitivity under impulsive loading. *J. Appl. Mech.* **31**, 38–42 (1964).
15. T. C. T. Ting, Large deformation of a rigid, ideally plastic cantilever beam. *J. Appl. Mech.* **32**, 295–302 (1965).
16. R. G. Hall, S. T. S. Al-Hassani and W. Johnson, The impulsive loading of cantilevers. *Int. J. Mech. Sci.* **13**, 415–430 (1971).
17. S. J. Hashmi, S. T. S. Al-Hassani and W. Johnson, Large deflexion elastic-plastic response of certain structures to impulsive load: numerical solutions and experimental results. *Int. J. Mech. Sci.* **14**, 843–860 (1972).
18. J. B. Martin, Impulsive loading theorems for rigid-plastic continua. *J. Engng Mech. Div. ASCE*, **EM5**, 27–42 (1964).
19. P. S. Symonds and C. T. Chan, Bounds for finite deflections of impulsively loaded structures with time-dependent plastic behaviour. *Int. J. Solids Structures* **11**, 403–423 (1975).
20. N. Jones, Dynamic behaviour of ideal fibre-reinforced rigid-plastic beams. *J. Appl. Mech.* **98**, 319–324, 1976.
21. E. W. Parkes and G. A. Carter, Dynamic thermal stresses in a pulsed reactor. *Phil. Trans. R. Soc. Lond.* **A270**, 325–347 (1971).
22. J. F. Ready, Effects due to absorption of laser radiation. *J. Appl. Phys.* **36**, 462–8 (1965).